Automated gold particle quantification of immunogold labeled micrographs

Rune Enger [a,b,*]

[a] Oslo University Hospital, Department of Neurology, N-0027 Oslo, Norway
[b] Letten Centre and GliaLab, Division of Physiology, Department of Molecular Medicine, Institute of Basic Medical Sciences, University of Oslo, N-0317 Oslo, Norway

HIGHLIGHTS

- A MATLAB toolbox for analyses of immunogold labeled micrographs is presented.
- Particle detection is based on multi-level thresholding, size and circularity.
- 97% of particles were detected on a large dataset with 0.1% false-positive rate.

ARTICLE INFO

ABSTRACT

Background: Immunogold cytochemistry is the method of choice for precise localization of antigens on a subcellular scale. The process of immunogold quantification in electron micrographs is laborious, especially for proteins with a dense distribution pattern.
New methods: Here I present a MATLAB based toolbox that is optimized for a typical immunogold analysis workflow. It combines automatic detection of gold particles through a multi-threshold algorithm with manual segmentation of cell membranes and regions of interests.
Results: The automated particle detection algorithm was applied to a typical immunogold dataset of neural tissue, and was able to detect particles with a high degree of precision. Without manual correction, the algorithm detected 97% of all gold particles, with merely a 0.1% false-positive rate.
Comparisons with existing method(s): To my knowledge, this is the first free and publicly available software custom made for immunogold analyses. The proposed particle detection method compares favorably to previously published algorithms.
Conclusions: The software presented here will be valuable tool for researchers in neuroscience working with immunogold cytochemistry.

1. Introduction

Quantitative immunogold cytochemistry has paved the way for a deeper understanding of the subcellular distribution of proteins and signaling substances in the central nervous system. No other method has got a comparable resolution – and although super resolution fluorescence imaging techniques are emerging as powerful alternatives – immunogold cytochemistry is still the method of choice for precise localization of proteins of interest in the nano domain scale.

Immunogold cytochemistry is a laborious process that comprises tissue fixation and embedding, followed by sectioning and subsequent labeling. For a detailed description see Mathiisen et al. (2006). In short, the labeling process involves optimizing antigenicity of the tissue and subsequently incubating the slices with antibodies towards the protein of interest. Secondary antibodies coupled to gold particles, recognizing the bound primary antibodies are then added. These are electron-dense, i.e. they appear as black dots on the resulting images. After labeling, electron micrographs are obtained and subsequently analyzed. The analyses comprise registering particle locations as well as manually defining cell membranes or cellular compartments, typically followed by calculation of gold particle densities per area or per length of cell membrane. Manual analyses of such data may be extremely time consuming, especially for densely labeled sections.

* Correspondence to: Department of Molecular Medicine, Institute of Basic Medical Sciences, University of Oslo, P. O. Box 1103, Blindern, N-0317 Oslo, Norway.
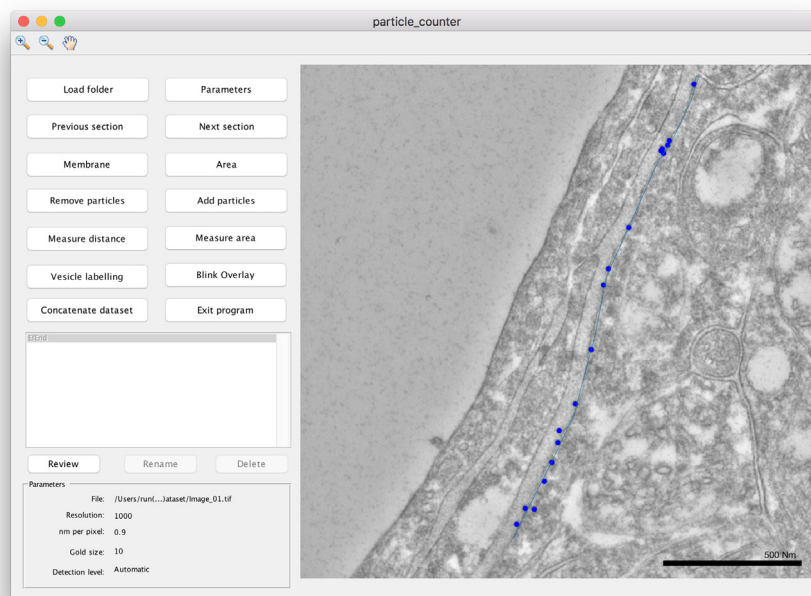E-mail address: rune.enger@medisin.uio.no

Fig. 1. Graphical user interface.

A few particle detection algorithms for immunogold labeled micrographs have been proposed. The most commonly applied method deploys a particle detector based on difference of gaussians (DoG) filtering followed by detection of local maxima, combined with either hessian testing or machine learning algorithms (Płaczek et al., 2015; Sousa et al., 2015; Wang et al., 2011). During preliminary trials with the current dataset, such particle detectors produced excellent results on some images, but was vulnerable to detection of non-gold particle structures with high local contrast. Simple thresholding algorithms have also been proposed (Lebonvallet et al., 1991), but with such methods, the threshold frequently needs to be modified by the analyzer to compensate for varying gray scale distribution of the micrographs and artifacts.

Membrane bound antigens pose a particular challenge for immunogold labeling as the combined size of the antibodies is large and detectable on the resolution scale electron micrographs are obtained (Ottersen, 1989). Hence, particles within a certain distance of the membrane should be considered as potential membrane labeling and should be included in the analyses (Mathiisen et al., 2006). Furthermore, it is necessary to evaluate labeling intensities at farther distances from the cell membrane to demonstrate whether or not there is an increased signal surrounding the membrane compared to the overall background labeling.

Similarly, labeling of small intracellular compartments like synaptic vesicles, poses an analytical challenge. In these cases, the size of the antibodies combined is larger than the structure in question. For these instances, a typical analysis comprises manually defining the center of the vesicles followed by detection of gold particles. Subsequently, the distribution of distances from synapses to the observed gold particles, is compared to the distribution of distances given randomly placed particles (Gundersen et al., 1998).

Here, I present a MATLAB based graphical user interface for automatic quantification of gold particle distribution by area or in relation to membrane segments or small intracellular structures in single-labeled or double-labeled electron micrographs. It is tailored to optimize a typical immunogold quantification workflow. The gold particle detection algorithm is fast and accurate, and comprises image optimization and standardization followed by automated multi-level thresholding.

2. Methods

The program consists of a MATLAB graphical user interface for analyses of micrographs, reviewing results and concatenating the final results (Fig. 1). The visual layout was created in MATLAB GUIDE toolbox in MATLAB 2016b and the program is tested on the MATLAB 2016b for Mac and Windows. The program is dependent on the MATLAB Image Processing Toolbox[TM]. The core functions of the program are written in object-oriented code and built-in functions in MATLAB have been chosen whenever available to ensure fast and reliable performance.

2.1. Organization of data

Images should be stored as tagged image file format (TIFF) files in folders according to subject or section, and the image resolution should result in a minimum gold particle diameter of at least 15–20 pixels to enable a high degree of automated particle detection. The results from the analyses will be stored in the same folder as the micrographs in a MATLAB data structure. This enables easy review and modification of the dataset if necessary.

2.2. Loading images and defining parameters

First, nanometers per pixel, gold size(s), magnification and gold particle detection method should be defined in the software ('Parameters'). Next, the user needs to select the working folder where the TIFF images are stored, before being prompted to choose which image to start analyzing.

2.3. Membrane or area segmentation (Fig. 4)

Subsequently, the user may draw a membrane line segment ('Membrane') or a region of interest ('Area') by use of a polygon tool, before indicating the intracellular side of the cell membrane and assigning the membrane a label and group. For quantifying gold particles associated with small cellular structures, the program is equipped with a function that allows the user to manually
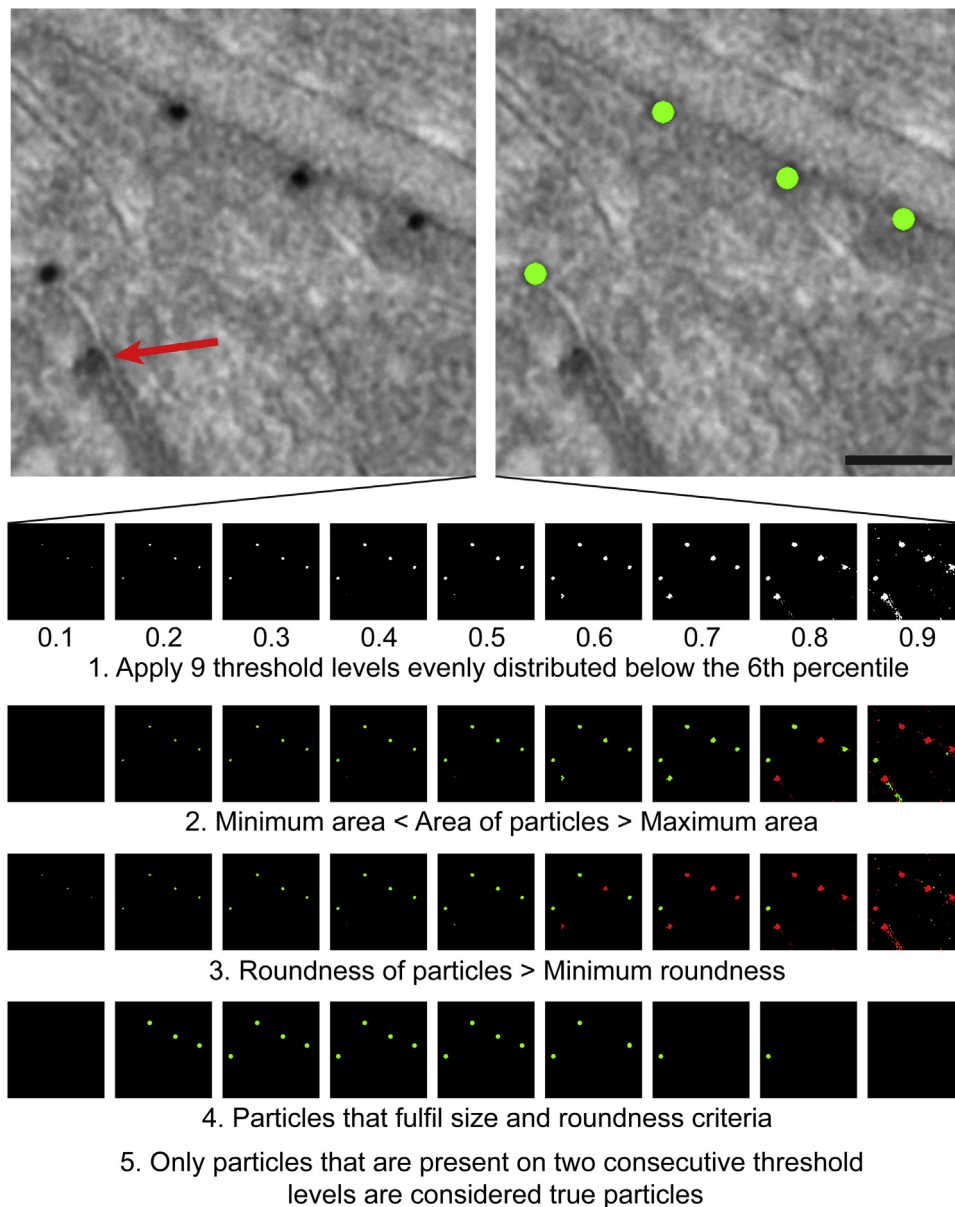
0.1 0.2 0.3 0.4 0.5 0.6 0.7 0.8 0.9
1. Apply 9 threshold levels evenly distributed below the 6th percentile

2. Minimum area < Area of particles > Maximum area

3. Roundness of particles > Minimum roundness

4. Particles that fulfil size and roundness criteria

5. Only particles that are present on two consecutive threshold levels are considered true particles

Fig. 2. Particle detection process. For the current dataset, nine thresholds, evenly spaced below the 6th percentile of gray level values, are applied to the micrographs. The connected components in the resultant binary images are tested on both size criteria and circularity. Green regions fulfill the respective criteria. Putative particles need to be classified as a proper particle in at least two consecutive threshold levels. These parameters ensure that structures that resembles gold particles are not detected (red arrow). Scale bar: 100 nm. (For interpretation of the references to color in this figure legend, the reader is referred to the web version of this article.)

mark these entities – e.g. synaptic vesicles – within an enclosed area selection. The distances from these structures to the detected particles are saved. Similarly, distances to the same number of randomly placed particles within the area are saved to allow the analyzer to reveal a clustering of particles relative to background labeling.

2.4. Particle detection (Fig. 2)

Three types of particle detection methods are provided with the toolbox: (1) Threshold-based particle detection based on size criteria with pre-set gray level thresholds ('Parameters' – 'Fixed threshold'), (2) threshold-based particle detection based on size criteria with interactive gray level thresholds ('Parameters' – 'Interactive'), and (3) fully automatic particle detection based on multi-level gray level thresholding ('Parameters' – 'Automatic'). The user may choose to detect gold particles of a single size, or gold particles of two different sizes. Common for all these meth-

ods is that the image background is normalized by local adaptive threshold filtering (MATLAB *adaptthresh()*) as the first step of the analysis.

2.4.1. Methods 1 and 2 – intensity threshold and size criteria

In 'Interactive' mode, the user should interactively try to mask out everything except the gold particles. Alternatively, in 'Fixed threshold' mode, a default (but adjustable) intensity value can be used, potentially minimizing the number of analyzer interactions per image. Subsequently, the built-in MATLAB function *regionprops()* is used to extract information on all connected components within a given size range. This provides the position of the centers of mass of all the detected particles. Only particles within a range of sizes are registered. For labeling with a single size of gold particle
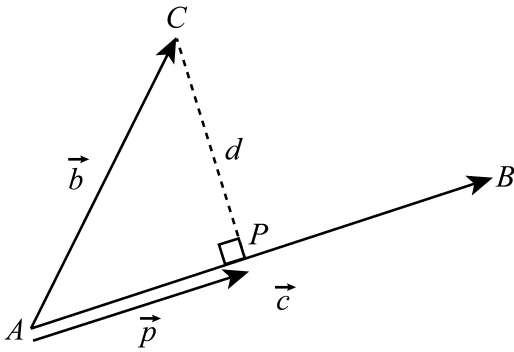
Fig. 3. The distance (d) from a particle (C) to a membrane segment (AB) is calculated.

the minimum and maximum areas (A) of particles are defined as follows:

$$A_{\min} = \pi \left(\frac{x \times d_{gold}}{2} \right)^2, \text{ where } x = 0.5 \text{ , for a single gold particle,} \quad (1)$$

and

$$A_{\max} = \pi \left(\frac{x \times d_{gold}}{2} \right)^2, \text{ where } x = 1.5, \text{ for a single gold particle,} \quad (2)$$

where d_{gold} is the diameter of the gold particles used, given in 'Parameters' and A represents the area of the particle in the image. For double-labeled sections, x values of 0.5 and 0.8 (Eq. (1)), and x values of 1.1 and 1.5 (Eq. (2)) is used for the smaller and larger gold particle sizes respectively. In addition, to improve detection specificity, regions within the defined area measurements need to meet certain circularity criteria. Circularity (C) is defined as follows, given the perimeter (P) and area (A) of the putative gold particle as detected with MATLAB *regionprops( )*:

$$C = \frac{(P_{\text{particle}})^2}{4\pi \times A} \quad (3)$$

2.4.2. Method 3 – Automatic particle detection based on multi-level thresholding

The gold particles are generally the darkest spots in the micrographs, and have a roughly circular shape, allowing thresholding-based algorithms to be effective. The problem, however, is to make a particle detection algorithm that works well on different datasets acquired on different setups and by different operators, without user intervention. To bypass these problems, the herein proposed method creates multiple thresholds within a range, and look through these for the best particle candidates. This range, specified from zero to a maximum percentile of the gray level distribution of the micrograph, and the number of threshold levels, are defined by the user in 'Parameters'. For the current dataset, nine thresholds were calculated below the 6th percentile of gray values in the micrograph. Tentative particles need to meet the size and circularity criteria, as above, but in addition to that, they need to be detected and classified as particles over two consecutive threshold levels (Fig. 2).

2.5. Membrane bound antigens

For membrane bound antigen labeling, the user should draw a one- or multi-segment line along the cell membrane in question (Fig. 4). The distance from each particle in the whole image to all segments of the drawn membrane is subsequently calculated, and the particles are assigned to their closest membrane segments. All particles within typically 20–25 nm of a line segment are saved as membrane bound particles. This distance is calculated according to the size of the gold particles being used and should match the theoretical combined size of primary and secondary antibodies plus

the radius of the gold particle (Mathiisen et al., 2006). The distances (d) from any particle's location (C) to a membrane segment (AB) are calculated (see Fig. 3). To find the shortest distance (d) from particle C to the line AB, first the projection point (P) of point C onto line AB is calculated:

$$\vec{P} = \vec{A} + \left(\frac{\vec{b} \cdot \vec{c}}{|\vec{c}|^2} \right) \vec{c}, \quad (4)$$

where $\vec{P} = (P_x, P_y)$ and $\vec{A} = (A_x, A_y)$. The ratio between $\vec{p}$ and $\vec{c}$ is calculated. For ratios between 0 and 1 the distance from the gold particle to the line segment equals the distance from C to P. For ratios below 0 or higher than 1, the point C does not project onto the line AB, and the shortest distance to the line is to point A or B respectively, as outlined below:

$$d_{PC} = \begin{cases} \sqrt{(C_x - A_x)^2}, & \frac{p}{c} \leq 0 \\ \sqrt{(C_x - P_x)^2}, & 0 < \frac{p}{c} < 1 \\ \sqrt{(C_x - B_x)^2}, & \frac{p}{c} \geq 1, \end{cases} \quad (5)$$

where p is the absolute value of $\vec{p}$ and c is the length of $\vec{c}$, which is defined as positive if $\vec{p}$ and $\vec{c}$ are parallell, and negative if $\vec{p}$ and $\vec{c}$ are antiparallell.

Particles that fall before the first line segment or after the last line segment, in case of an open-ended membrane segment, are excluded.

Additionally, all particles within 300 nm from the membrane segment are stored in a similar fashion to enable analyses of particle distribution relative to the cell membrane, with positive values indicating intracellular positions, and negative values indicating extracellular positions. The user is prompted to define the intracellular side of the membrane cell membrane.

2.6. Non-membrane bound antigens

The program also allows quantification of labeling within a region of interest ('Area'). Here, the user has to define an enclosed area instead of an open-ended membrane segment. If the particle is localized within the defined area, the locations for this particle is saved. This tool may also be used to register background labeling. As with the membrane bound antigen case, gold particles within 20–25 nm (see above) of the edge of the area are stored separately to allow analysis of membrane labeling of enclosed structures.

2.7. Adding or removing particles

To manually correct the automatically detected gold particles, the user may choose to add or remove gold particles. Adding particles is done by defining one or several points by mouse click (only points within the given distance boundaries are saved). Similarly, removing particles is done by clicking on – or very close to – one or several particles. There is a button to allow the user to blink the particle overlay, so that underlying image morphology becomes apparent (which facilitates removal of false-positives).

2.8. Measuring distances and areas

There is also a simple tool for measuring distances and areas in the micrographs. The user is prompted to define a line or area selection, respectively, and the program saves the length or area in μm or μm^2.
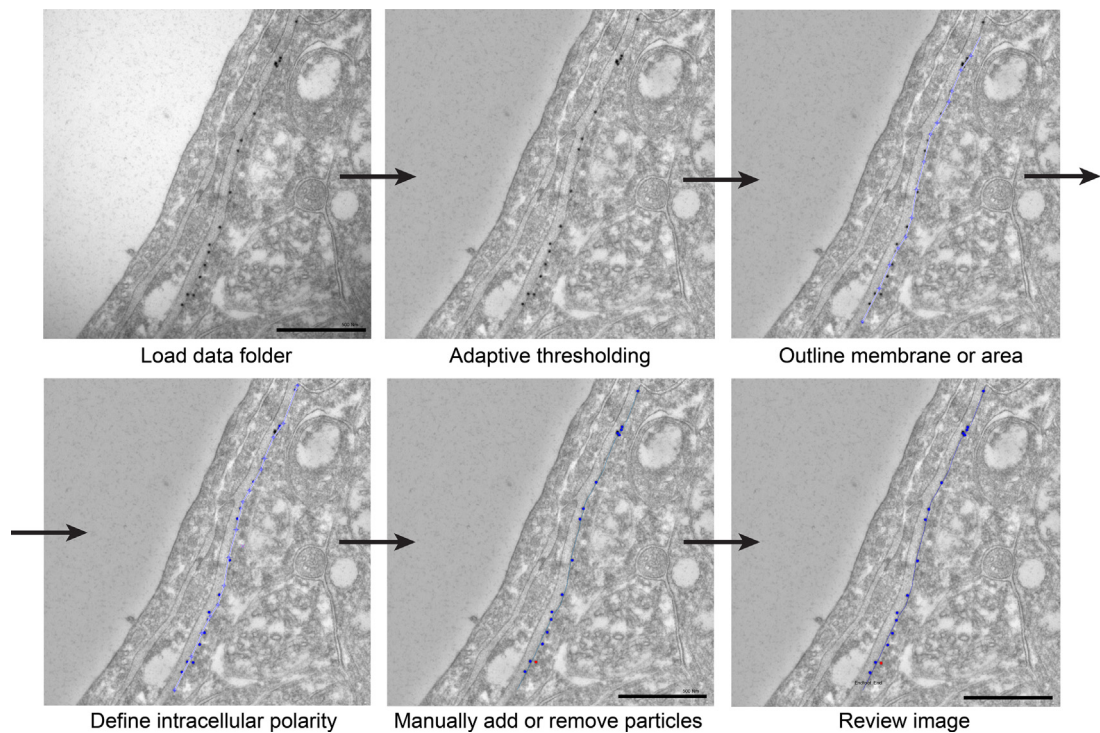
Fig. 4. Image analysis work-flow. (1) The analyses are initiated by selecting a folder and an image. (2) The images' background levels are normalized using a local adaptive thresholding filter. (3) Membranes or areas of interest are manually outlined by the analyst and the program detects the particles. (4) The intracellular side of the cell membrane is defined. (5) Particles are added or removed if needed. (6) The current or previously analyzed membrane segments or areas can easily be reviewed.

2.9. Review results

A review mode in the main graphical user interface enables the user to easily review membrane segments or area selections with their corresponding gold particles as well as area and distance measurements. In review mode, analyzed membranes, particles and areas may be deleted or renamed.

2.10. Tissue for method validation

Six male C57BL6/J mice (Charles River Laboratories, Sulzfeld, Germany), of at least 8 weeks of age were included in the study. The animals were allowed ad libitum access to food and drinking water. All experiments were approved by the institution's Animal Care and Use Committee. Animals were anesthetized by an i.p. injection of a mixture of chloral hydrate, magnesium sulfate and pentobarbital (142, 70, and 32 mg/kg, respectively). Brain tissue was fixed by transcardiac perfusion (10 mL/min) with 0.2% 70,000 Da dextran in phosphate buffer, followed by phosphate-buffered 4% formaldehyde containing 0.1% glutaraldehyde. For immunogold cytochemistry, small blocks of fixed cortex were subjected to freeze substitution and infiltration in Lowicryl HM20 resin (Polysciences, Warrington, PA, Cat 15924), before labeling with primary and secondary antibodies. Sections were incubated sequentially in the following solutions (at room temperature): (1) 50 mM glycine in 6 mM Tris buffer containing 0.01% Triton X-100 and 50 mM NaCl (TBST; 10 min); (2) 0.2% milk powder in TBST (10 min); (3) primary antibody (anti-AQP4 from Sigma, 1.5 μg/mL) diluted in the solution used in the preceding step (overnight); (4) same solution as in step 2 (10 min × 2); (5) gold-conjugated IgG (GAR15 nm; Abcam, Cambridge, UK), diluted 1:20 in TBST containing milk powder and polyethylene glycol (0.5 mg/mL, 1 h). Finally, the sections were counterstained and examined in a FEI Tecnai 12 transmission electron microscope (FEI Company, Hillsboro, OR). Images were recorded at a nominal magnification of 43,000×, in 1376 × 1032 pixels, 8-bit TIFF images.

3. Results

To validate the particle detection algorithm, a typical immunogold dataset was analyzed, containing 311 electron micrographs from mouse cerebral cortex, labeled with antibodies toward the water channel aquaporin-4, which is abundantly expressed in the astrocytic endfoot processes abutting the vasculature (Fig. 5, Nagelhus and Ottersen, 2013). In total 1126 μm of astrocytic cell membrane was analyzed.

A high density of gold particles signifying aquaporin-4 water channels were centered on the membranes facing the endothelial cells, as previously shown (Fig. 5A, Enger et al., 2012). In all, 10924 particles were detected automatically; 371 particles needed to be added manually (3.4% of total), and 14 particles had to be removed (0.1% of total). The average density of gold particles along the cell membranes facing the vasculature was 5.43 ± 0.12 gold particles per μm (Fig. 5B). The corresponding value for the membrane of the astrocyte facing the neuropil was 0.62 ± 0.05 particles per μm. Hence, the membranes facing the vasculature accommodated a roughly 9-fold higher density of aquaporin-4 compared to the membrane facing the neuropil ($p < 0.001$, $n = 309$ segments facing the vasculature, 287 facing the neuropil from 13 sections, 6 mice, Welch's t-test).

Particles within 300 μm of the cell membranes were saved to evaluate background labeling. When the distance from the cell membrane for any given particle was plotted in a histogram centered on the cell membrane, a pronounced membrane centered signal became evident (Fig. 5C).

To evaluate the particle detectors ability to detect two different classes of gold particles, a mock dataset of 30 micrographs with gold particles separated by a factor of two was created. The detector is still able to detect 97% of the smaller gold particles and 84% of
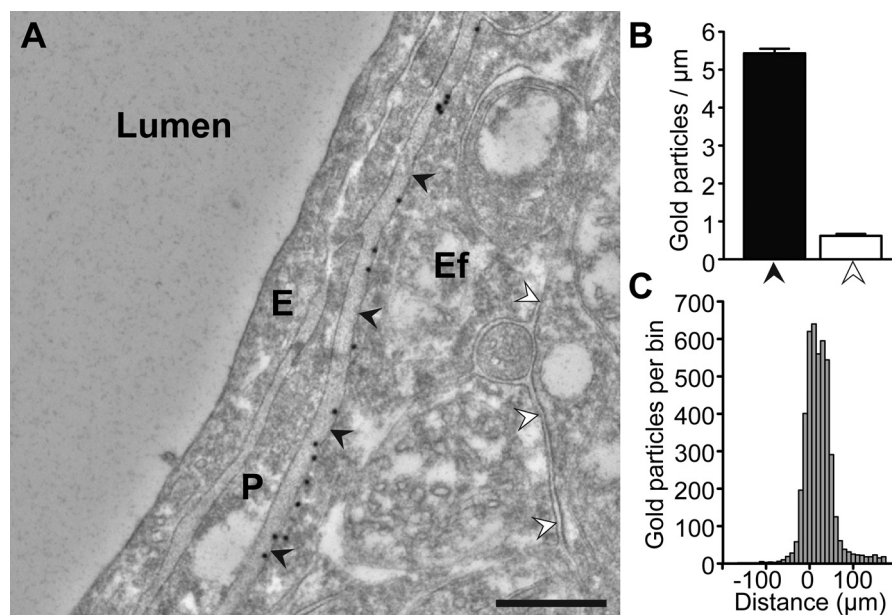
Fig. 5. (A) Aquaporin-4 labeling of perivascular astrocytic endfeet surrounding a capillary. E = endothelium, P = pericyte and Ef = endfoot process. Black arrowheads: astrocyte membrane facing the blood vessel. White arrowheads: astrocytic membranes facing the neuropil. (B) Mean particle density ± s.e.m. along the two membrane domains (same color code as A). (C) Distribution of gold particles labeling aquaporin-4 along an axis perpendicular to the perivascular endfoot membrane. The ordinate indicates numbers of gold particles per bin (bin width, 10 nm; cytoplasmic side positive). Scalebar: 500 nm.

the larger gold particles. Only 6% of the small particles had to be removed manually, while no large particles needed to be removed.

4. Discussion

Immunogold cytochemistry remains the method of choice for detailed analyses of subcellular antigen distribution. Here, I present a software toolbox that would significantly reduce time spent analyzing immunogold micrographs. Some key immunogold analysis techniques are included, and the program is optimized for an efficient workflow and easy review of results. The program has proven stable and efficient for analyzing a large immunogold dataset of more than 300 images. With fully automatic multi-level thresholding, the program detects nearly all particles, and the method has a very low false-positive rate (see Section 3). A function for easily and quickly adding or removing particles is provided.

Six images in the dataset were excluded as no particles were detected. This was a result of a strongly skewed distribution of gray level values in these images – typically a result of parts of the metal grid supporting the specimen appearing on the micrograph. In such cases, manual adjustment of threshold would be the preferred action. One cannot rule out that other microscopes and operators would produce datasets with markedly different gray value distribution, but the procedure has been applied to images obtained on three different electron microscopes with different magnifications and resolution settings. If the automated detection fails on a larger portion of micrographs of a dataset, the range for the automated thresholding could be adjusted.

Particles that are not detected with the present algorithm, are typically clusters of particles that are so closely situated that thresholding can not be used for separation. A method that could also detect such conglomerates of particles would more likely be based on circle hough transform (Illingworth and Kittler, 1987) or finding local extrema in difference-of-gaussian filtered images (Wang et al., 2011). In our hands, however, the uniqueness of the particles, compared to the relative strongly contrasted cell membranes in the present dataset, seems to decline using the above mentioned methods, ultimately producing higher false-positive rates. Multi-

ple closely situated particles may also be a result form clustering of gold particles, and not represent two close epitopes being labeled, and one could argue that these particles should be left out from the analyses altogether (Bergersen et al., 2008).

Manually segmenting curved cell membranes by a multi-segment line tool could introduce errors if too few sub-segments are defined. To enable precise manual segmentation, regions of the micrograph may be magnified while outlining the membrane.

Ideally, all the analyses – including membrane and area segmentation – would have been fully automated. Advanced algorithms have been created that could perform such membrane segmentation (Kreshuk et al., 2011, 2014). However, cell membrane contrast in tissue prepared for immunogold cytochemistry is often not of good enough for automatic segmentation of membrane sections or cellular structures, as there is a trade-off between the strength of tissue fixation and labeling efficacy (Mathiisen et al., 2006).

5. Conclusion

To my knowledge, no publicly available software performing automated particle detection in combination with area and membrane selections is available. The toolbox presented here will be a valuable tool for researchers in neuroscience working with immunogold cytochemistry.

6. Download

A link to download the newest version of the program is provided on request (rune.enger@medisin.uio.no).

References

Bergersen, L.H., Storm-Mathisen, J., Gundersen, V., 2008. Immunogold quantification of amino acids and proteins in complex subcellular compartments. Nat. Protoc. 3, 144–152.

Enger, R., Gundersen, G.A., Haj-Yasein, N.N., Eilert-Olsen, M., Thoren, A.E., Vindedal, G.F., Petersen, P.H., Skare, O., Nedergaard, M., Ottersen, O.P., Nagelhus, E.A., 2012. Molecular scaffolds underpinning macroglial polarization: an analysis of retinal Muller cells and brain astrocytes in mouse. Glia 60, 2018–2026.

Gundersen, V., Chaudhry, F.A., Bjaalie, J.G., Fonnum, F., Ottersen, O.P., Storm-Mathisen, J., 1998. Synaptic vesicular localization and exocytosis of L-aspartate in excitatory nerve terminals: a quantitative immunogold analysis in rat hippocampus. J. Neurosci. 18, 6059–6070.

Illingworth, J., Kittler, J., 1987. The adaptive hough transform. IEEE Trans. Pattern Anal. Mach. Intell. 9, 690–698.

Kreshuk, A., Straehle, C.N., Sommer, C., Koethe, U., Cantoni, M., Knott, G., Hamprecht, F.A., 2011. Automated detection and segmentation of synaptic contacts in nearly isotropic serial electron microscopy images. PLoS One 6 (10), e24899.

Kreshuk, A., Koethe, U., Pax, E., Bock, D.D., Hamprecht, F.A., 2014. Automated detection of synapses in serial section transmission electron microscopy image stacks. PLoS One 9 (2), e87351.

Lebonvallet, S., Mennesson, T., Bonnet, N., Girod, S., Plotkowski, C., Hinnrasky, J., Puchelle, E., 1991. Semi-automatic quantitation of dense markers in cytochemistry. Histochemistry 96, 245–250.

Mathiisen, T.M., Nagelhus, E.A., Jouleh, B., Torp, R., Frydenlund, D.S., Mylonakou, M.-N., Amiry-Moghaddam, M., Covolan, L., Utvik, J.K., Riber, B., 2006. Postembedding immunogold cytochemistry of membrane molecules and amino acid transmitters in the central nervous system. In: Neuroanatomical Tract-Tracing 3. Springer, pp. 72–108.

Nagelhus, E.A., Ottersen, O.P., 2013. Physiological roles of aquaporin-4 in brain. Physiol. Rev. 93, 1543–1562.

Ottersen, O.P., 1989. Quantitative electron microscopic immunocytochemistry of neuroactive amino acids. Anat. Embryol. (Berl.) 180, 1–15.

Płaczek, B., Bułdak, R.J., Brenk, A., Polaniak, R., 2015. Automatic evaluation of area-related immunogold particles density in transmission electron micrographs. In: Asian Conference on Intelligent Information and Database Systems, Springer International Publishing, pp. 53–61.

Sousa, R.G., Esteves, T., Rocha, S., Figueiredo, F., Quelhas, P., Silva, L.M., 2015. Automatic detection of immunogold particles from electron microscopy images. In: International Conference Image Analysis and Recognition, Springer International Publishing, pp. 337–384.

Wang, R., Pokhariya, H., McKenna, S.J., Lucocq, J., 2011. Recognition of immunogold markers in electron micrographs. J. Struct. Biol. 176, 151–158.